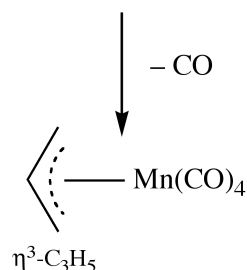
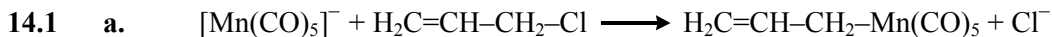
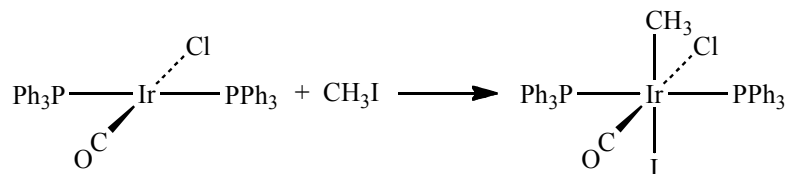


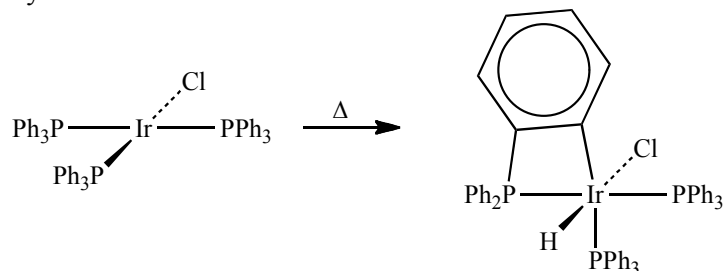
CHAPTER 14: ORGANOMETALLIC REACTIONS AND CATALYSIS



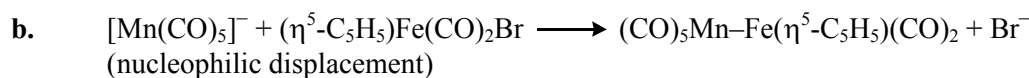
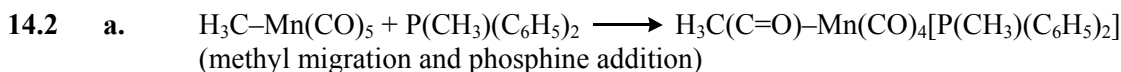
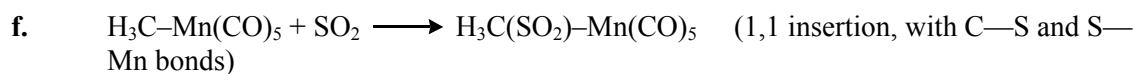
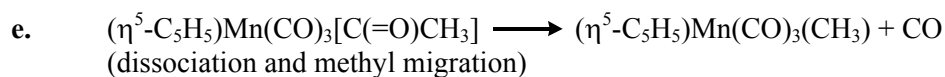
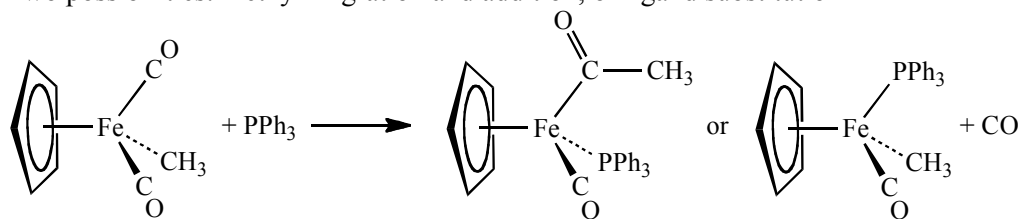
b. Oxidative addition

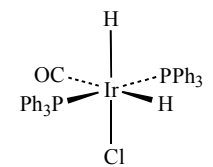
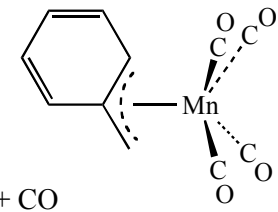
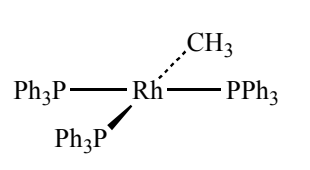
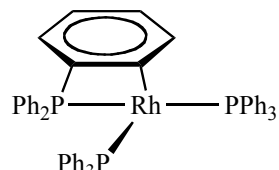


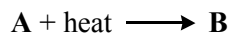
c. Cyclometallation



d. Two possibilities: methyl migration and addition, or ligand substitution

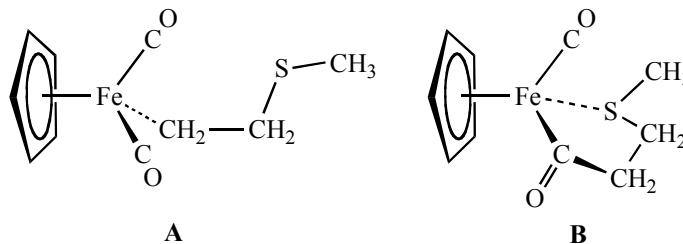


- c. $\text{trans-Ir(CO)Cl(PPh}_3)_2 + \text{H}_2 \longrightarrow$ 
- d. $\text{W(CO)}_6 + \text{C}_6\text{H}_5\text{Li} \longrightarrow [\text{C}_6\text{H}_5\text{COW(CO)}_5]^- + \text{Li}^+$ (nucleophilic attack on carbonyl C)
- e. Alkyl migration of CH_3 to one of the adjacent CO ligands, followed by addition of ^{13}CO . Isomeric products: 1/3 each of the *fac* enantiomers, 1/3 *mer* isomer. There should be no ^{13}C in the acyl group.
- f. Alkyl migration of CH_3 to one of the adjacent CO ligands, followed by addition of ^{13}CO . Isomeric products: two *mer* species, enantiomers if the ^{13}CO is taken into account, identical otherwise.
- 14.3 a. $\text{cis-}(^{13}\text{CO})(\text{CH}_3\text{CO})\text{Mn(CO)}_4 \longrightarrow \text{Mn(CH}_3\text{)(CO)}_5$, 25% with no ^{13}CO , 25% with ^{13}CO *trans* to CH_3 , 50% with ^{13}CO *cis* to CH_3 .
- b. $\text{C}_6\text{H}_5\text{-CH}_2\text{Mn(CO)}_5 \xrightarrow{h\nu} \text{CO} +$ 
- c. $[\text{V(CO)}_6] + \text{NO} \longrightarrow [\text{V(CO)}_5(\text{NO})] + \text{CO}$
- d. $\text{Cr(CO)}_6 + 2 \text{Na/NH}_3 \longrightarrow 2 \text{Na}^+ + [\text{Cr(CO)}_5]^{2-} + \text{CO}$
- e. $\text{Fe(CO)}_5 + \text{NaC}_5\text{H}_5 \longrightarrow \text{Na}^+ + [(\eta^5\text{-C}_5\text{H}_5)\text{Fe(CO)}_2]^- + 3 \text{CO}$
- f. $[\text{Fe(CO)}_4]^{2-} + \text{CH}_3\text{I} \longrightarrow [(\text{CH}_3)\text{Fe(CO)}_4]^- + \text{I}^-$
- g.  $\xrightarrow{\Delta} \text{CH}_4 +$ 
- 14.4 $[(\text{C}_5\text{H}_5)\text{Fe(CO)}_3]^+ + \text{NaH} \longrightarrow \text{A (C}_7\text{H}_6\text{O}_2\text{Fe)}$ $\text{A} = (\eta^5\text{-C}_5\text{H}_5)\text{Fe(CO)}_2\text{H}$
- $\text{A} \longrightarrow \text{B (colorless gas)} + \text{C (C}_7\text{H}_5\text{O}_2\text{Fe) (purple-brown)}$ $\text{B} = \text{H}_2$
- (See Figure 13.35, p. 509 for structure of C.) $\text{C} = [(\eta^5\text{-C}_5\text{H}_5)\text{Fe(CO)}_2]_2$
- $\text{C} + \text{I}_2 \longrightarrow \text{D (C}_7\text{H}_5\text{O}_2\text{FeI) (brown)}$ $\text{D} = (\eta^5\text{-C}_5\text{H}_5)\text{Fe(CO)}_2\text{I}$
- $\text{D} + \text{TiC}_5\text{H}_5 \longrightarrow \text{E (C}_{12}\text{H}_{10}\text{O}_2\text{Fe)} + \text{TiI}$ $\text{E} = (\text{C}_5\text{H}_5)_2\text{Fe(CO)}_2$
- (See Figure 13.35, p. 509 for structure of E.) (one Cp η^1 and one Cp η^5)
- $\text{E} \longrightarrow \text{F (C}_{10}\text{H}_{10}\text{Fe)} + \text{colorless gas (CO)}$ $\text{F} = (\eta^5\text{-C}_5\text{H}_5)_2\text{Fe, ferrocene}$



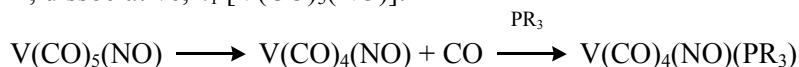
A has bands at 1980 and 1940 cm^{-1} , **B** at 1920 and 1630 cm^{-1} .

The sulfur reagent loses Cl^- and bonds to the Fe as an alkyl ligand to form **A**, with two carbonyls. This is an example of nucleophilic displacement of chloride by an organometallic anion. **A** then rearranges, with the S becoming attached to Fe, and the alkyl migrates to a carbonyl carbon. **B** contains an ordinary carbonyl and an acyl $\text{C}=\text{O}$ bond, for the two quite different $\text{C}-\text{O}$ stretching energies.



- 14.6 a. Two term rate laws like this could be the result of two parallel associative reactions—the first by solvent, the second by the phosphate—or could result from a dissociative reaction for the first term and an associative reaction for the second.

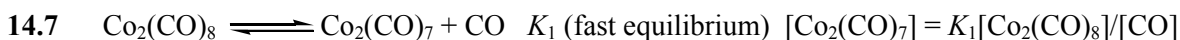
First term, dissociative, $k_1 [\text{V}(\text{CO})_5(\text{NO})]$:



Second term, associative, $k_2[\text{PR}_3][\text{V}(\text{CO})_5(\text{NO})]$:



- b. $\text{V}(\text{CO})_5[\text{P}(\text{OCH}_3)_3](\text{NO})$ If the NO is a bent, 1-electron donor, it can be an 18-electron species ($5 + 5 \times 2 + 2 + 1 = 18$). If the NO is a linear, 3-electron donor, the total is 20 electrons.



$$\text{Rate} = k_2[\text{Co}_2(\text{CO})_7][\text{H}_2] = k_2K_1 [\text{Co}_2(\text{CO})_8][\text{H}_2]/[\text{CO}]$$

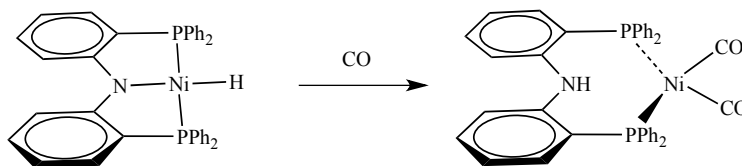
- 14.8 This depends on the cone angle of the phosphine ligands, with the order $\text{PPh}_3 > \text{PBu}_3$ (estimated) $> \text{P}(\text{OPh})_3 > \text{P}(\text{OMe})_3$ from Table 14.1 (p. 543). The PPh_3 should dissociate most rapidly and the $\text{P}(\text{OMe})_3$ should dissociate least rapidly.

- 14.9 K for the dissociation reaction is in the order $\text{PPh}_3 > \text{PMePh}_2 > \text{PEt}_3 > \text{PMe}_3$, as a result of a combination of decreasing cone angle and increasing negative charge on the phosphorus. Alkyls push more electron density onto P than phenyl rings.

- 14.10 a.** Tolman employed Ni(0) complexes of general formula $\text{Ni}(\text{CO})_3(\text{PX}_1\text{X}_2\text{X}_3)$ where the substituents of the monodentate phosphine were varied.
- b.** The parameter χ was defined as follows to determine the energy of the $\text{Ni}(\text{CO})_3(\text{PX}_1\text{X}_2\text{X}_3)$ A_1 carbonyl stretching mode, with each phosphine substituent contributing a χ value. The 2056.1 cm^{-1} relatively low energy ν_{CO} absorption is the A_1 mode of $\text{Ni}(\text{CO})_3(\text{P}^t\text{Bu}_3)$, containing the strong σ -donor P^tBu_3 .

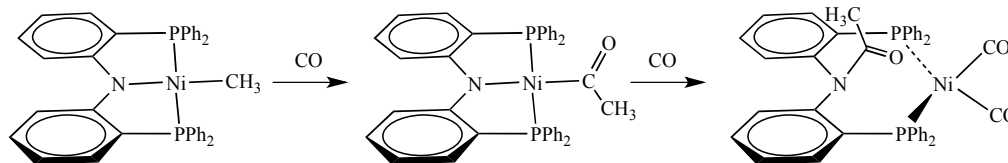
$$\nu_{\text{CO}}(A_1) = 2056.1 + \sum_{i=1}^3 \chi \text{ cm}^{-1}$$

- c.** These χ values range from 0 to 19.6 cm^{-1} , with the highly electronegative Cl (14.8), F (18.2) and CF_3 (19.6) substituents contributing the most towards shifting the A_1 carbonyl stretching mode to higher energy.
- d.** The debate over the classification of phosphine ligands as σ -donors and π -acceptors is discussed in this reference. Tolman states that while highly electronegative substituents have higher χ values (and cause higher energy ν_{CO} absorptions) and more electron-donating substituents have lower χ values, the relative importance of σ donation and π acceptance for these phosphine-nickel bonds is difficult to assess.
- 14.11 a.** The conversion of the Ni(II) complex to a Ni(0) complex is shown here:



Upfield-shifted metal-hydride ^1H resonances are common. In this reaction, the Ni—H resonance (-18 ppm) is replaced by one at 8.62 ppm , consistent with formation of the secondary amine. Two carbonyl absorptions are consistent with the *cis* carbonyl product shown. The authors speculate that the first step in this reaction is CO coordination at Ni(II) to afford a five coordinate intermediate that presumably brings the amido nitrogen and the hydride into *cis* positions. Reductive elimination results in N—H bond formation. Initial CO binding renders the Ni(II) center more electrophilic (via π -backbonding) and a better oxidizing agent. CO binding also generates a five-coordinate complex with the amido nitrogen and the hydride in closer proximity to facilitate the orbital overlap necessary for reductive elimination.

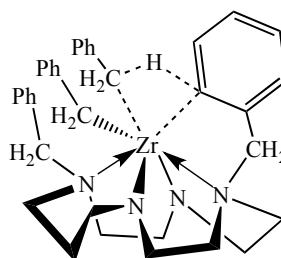
- b. The alternate reaction pathway exhibited by the Ni—CH₃ complex is:



The first reaction is proposed as a migratory insertion of CO into the Ni—CH₃ bond, affording an acyl complex with a diagnostic 1621 cm⁻¹ carbonyl absorption. Further reaction with CO results in reductive elimination of a N—C_{sp²} bond and formation of a neutral amide-functionalized bidentate phosphine ligand. As in Part **a**, the first step in the reductive elimination reaction is hypothesized as CO coordination at Ni(II) of the intermediate, resulting in a five-coordinate species with the amido nitrogen atom and the acyl ligand carbon atom in close proximity.

- c. The interesting feature of the Part **b** scheme is that no N—C_{sp³} bond formation occurs when CO is added to the Ni—CH₃ complex. The authors of the reference primarily attribute this to an electronic effect. The more electron-rich Ni(II) center in the Ni—CH₃ complex is less reactive towards reductive elimination compared to the less electron-rich Ni(II) center in the Ni—H complex. Note that these reductive eliminations are proposed to begin via initial coordination of CO, rendering the metal center more electrophilic for subsequent reductive elimination by virtue of π -backbonding. In these reductive elimination reactions, Ni(II) formally serves as the oxidizing agent (it goes from Ni(II) to Ni(0)); a less electron-rich Ni(II) would be expected to be a better oxidizing agent. An idea not mentioned in the reference is that activation barriers for reductive eliminations involving H atoms are generally lower than those involving CH₃ groups (leading to faster reductive elimination rates with H atoms). The spherical symmetry of the 1s H orbital better facilitates effective overlap throughout reductive elimination pathways when compared to the *sp*³ hybrid orbital employed by a methyl group.

- 14.12 a. This double-cyclometallation very likely occurs via σ -bond metathesis. A sketch of a possible four-centered transition state (compare to the general σ -bond metathesis transition state in Figure 14.8) is shown below. This structure presumably leads to toluene expulsion with concomitant orthometallation of the aromatic ring.



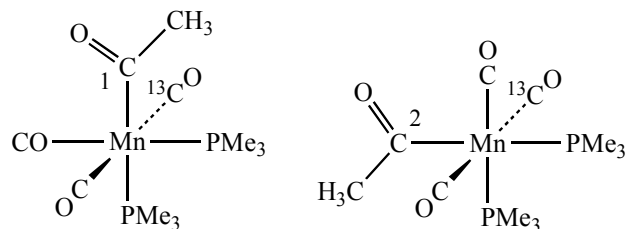
- b. Since Zr(IV) is in its highest oxidation state, and is not electronically predisposed to participate in sequential oxidative addition/reductive elimination steps to affect orthometallation via metal hydride intermediates, a σ -bond metathesis pathway seems like the best choice. The rate of this *intramolecular* process would be expected

independent of H_2 pressure. This pathway includes neither the release of hydrogen gas nor hydride intermediates that could arise from hydrogen gas.

The reference does not speculate as to why the rate with $R = CH_2Ph$ is the slowest. It is possible that the steric bulk of the four aromatic rings in the proposed transition state structure may raise the activation barrier for formation of the four-centered transition state, decreasing the reaction rate.

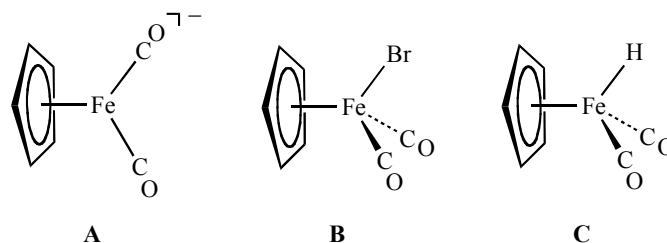
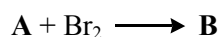
- 14.13** If it loses CO followed by migration of CH_3 to an adjacent position, all the CO lost should be ^{12}CO , because the CO ligands *cis* to the $CH_3C=O$ will be the ones lost.

- 14.14 a.** There are two possible products, both a result of methyl migration followed by carbonyl addition. The methyl group can move to either the 1 position or the 2 position. The resulting products are different only in the location of the ^{13}CO .



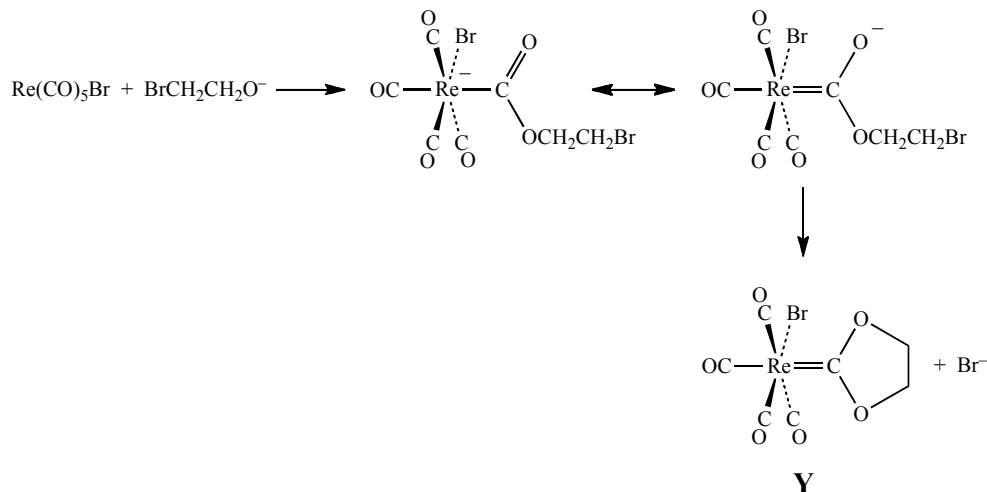
- b.** The new IR band is from the acyl carbonyl, and should be near 1630 cm^{-1} (see Problem 14.5).

- 14.15** $[(C_5H_5)_2Fe_2(CO)_4] + Na/Hg \longrightarrow A$



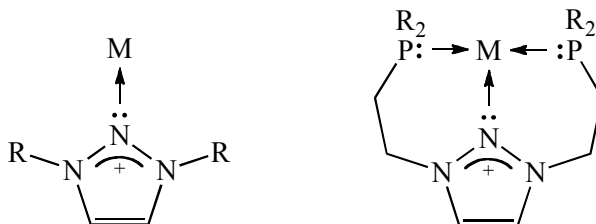
- A:** Sodium acts as reducing agent. Anion **A** has lower energy C–O stretches, as expected (see p. 488).
B: Br_2 acts as oxidizing agent and is the source of the bromo ligand.
C: The NMR peak at -12 ppm is caused by the hydride ligand.
D: benzene, C_6H_6

- 14.16 a.** The bromoethoxide anion adds to a carbonyl; the hard oxygen of the anion adds to the hard carbon. Then Br^- is lost, leaving a positive carbon. The alkyl tail can then bend around and react with the carbonyl oxygen, giving the compound shown here:



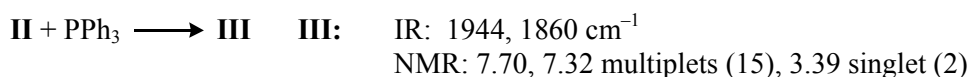
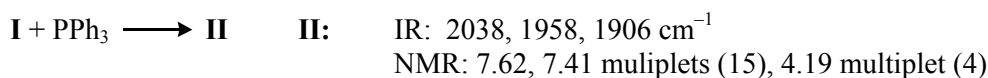
b. There are 2 electrons donated from each of the six ligand positions, and Re^+ has 6 electrons for a total of 18. In the isomer shown, there are three different carbonyls, and the carbene ligand has two identical carbons, so there are five different magnetic environments for carbon. In the other possible isomer, with Br trans to the alkoxide ligand, there are not five different carbon environments. Finally, Ag^+ can remove Br^- from the complex.

14.17 Nitrenium ligands are similar to N-heterocyclic carbene (NHC) ligands (see Figure 14.33(a)) except that they have a nitrogen atom in place of the coordinating carbon; three nitrogens are in a row. R groups that have been studied include those with phosphine arms that can also coordinate to metals.



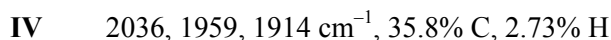
Nitrenium ligands have been demonstrated to be weaker sigma donors than NHC ligands on the basis of infrared and bond length evidence, supported by density functional theory calculations; see the reference for details. The phosphine arms that also coordinate to metals give nitrenium ligands pincer characteristics comparable to the ligands discussed in Section 14.1.5

14.18 a. This is the example described in Example 13.4, p. 531.



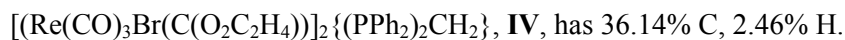
II has 3 CO ligands in a *fac* geometry. The NMR shows one PPh₃ (15) and the ethylene hydrogens (4).

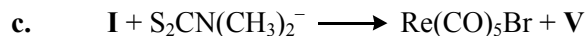
III has only 2 CO ligands in a *cis* configuration. The ratio of NMR integrated peaks is now 15:2 because there are two PPh₃ groups.



Replacing two CO's with the phosphine gives a compound with 25.7% C, 3.1% H. Replacing one CO and the Br with the phosphine gives a compound with 28.9% C, 3.3% H.

The only way to get the analysis to work out is to have a single diphos ligand bridging two Re atoms after loss of CO from each:

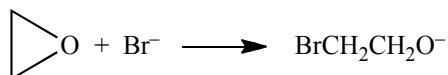




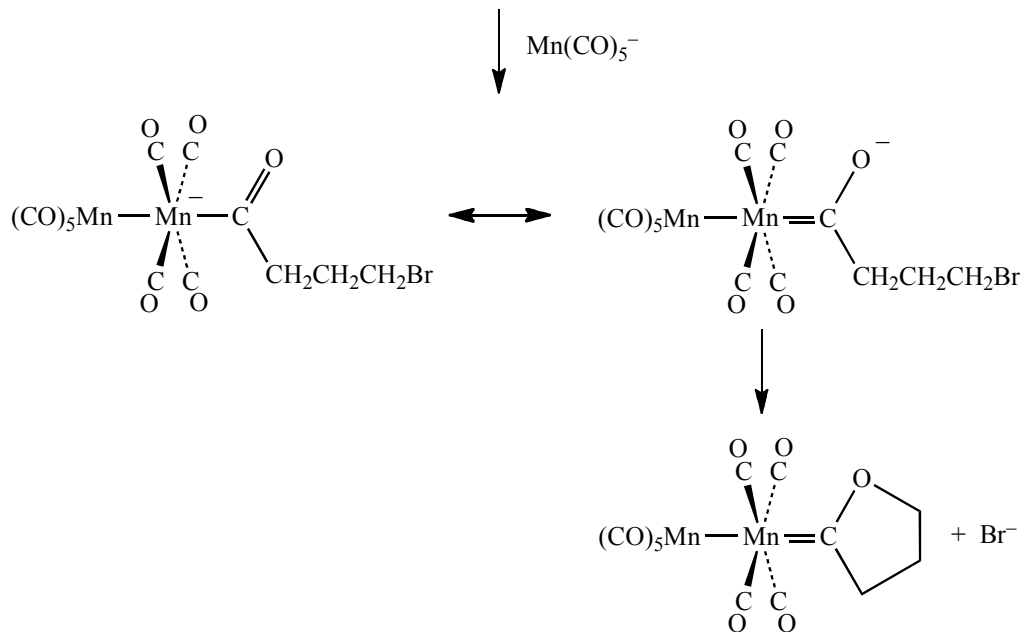
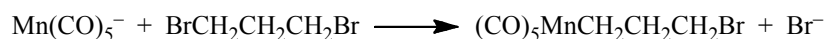
V has no metal, has no IR bands between 1700 and 2300 cm^{-1} , has NMR bands at 3.91 (triplet), 3.60 (triplet), 3.57 (singlet), and 3.41 (singlet).

Acting as a nucleophile, the dithiocarbamate ion attacks the carbene to form $(\text{CH}_3)_2\text{NC}(=\text{S})\text{SC}_2\text{H}_4\text{O}^-$, which can pick up a proton from trace amounts of water to make the hydroxy compound $(\text{CH}_3)_2\text{NC}(=\text{S})\text{SC}_2\text{H}_4\text{OH}$, V. The 1500 and 977 cm^{-1} bands are the N–C and C–S bands, and the NMR shows triplets for the two CH_2 units, singlets for the CH_3 's.

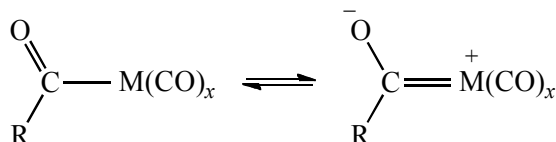
- 14.19 The mechanism is the one described in problem 16, with formation of the alkoxide ion by the reaction:



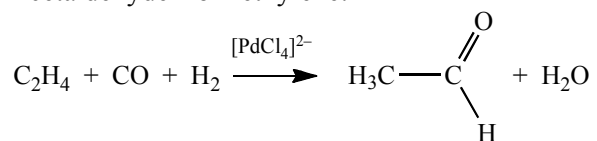
- 14.20 The reaction proceeds by substitution of $\text{Mn}(\text{CO})_5^-$ for Br^- , followed by alkyl migration, addition of $\text{Mn}(\text{CO})_5^-$, and finally cyclization:



- 14.21 The acyl metal carbonyl has a resonance structure with a negative charge on oxygen, shown below, where the proton can add. Protonation is then similar to the alkylation reaction described in Section 13.6.2.

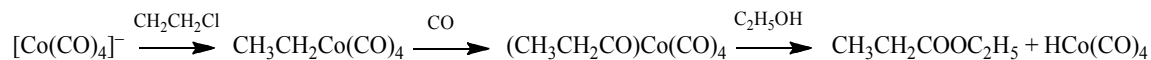


- 14.22 a.** Acetaldehyde from ethylene:



The Wacker process (Figure 14.21) with ethylene as the starting alkene will result in acetaldehyde.

- b.** Ethyl propionate from chloroethane:



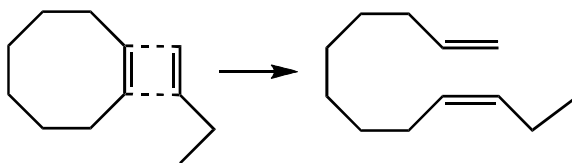
- c.** Pentanal from 1-butene: The hydroformylation process (Figure 14.18) does this.
- d.** 4-phenylbutanal from an alkene: Again, the hydroformylation process should do this, starting with 4-phenyl-1-propene.
- e.** Wilkinson's catalyst $[\text{ClRh}(\text{PPh}_3)_3]$ (Figure 14.22) should do this. D_2 would be added across the least hindered double bond.
- f.** Catalytic deuteration with H_3TaCp_2 (Figure 14.17) should deuterate the phenyl ring without affecting the methyl hydrogens.

- 14.23** Figure 14.19 shows this process of hydroformylation. *n*-pentanal results if $\text{R} = \text{C}_2\text{H}_5$. Identification of the steps:

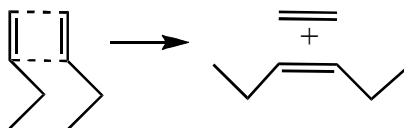
1. Dissociation of one CO
2. Addition of the alkene
3. 1,2 insertion
4. Addition of CO
5. Alkyl migration
6. Oxidative addition
7. Reductive elimination of the aldehyde

- 14.24** Hydroformylation (Figure 14.19) with $\text{Rh}(\text{CO})_2(\text{PPh}_3)_2$ as the catalytic species will work, starting with 2-methyl-1-butene: $\text{H}_3\text{C}-\text{CH}_2-\text{C}(\text{CH}_3)=\text{CH}_2$.

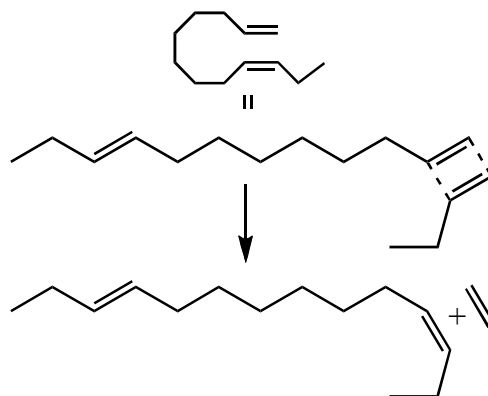
14.25 a. Direct metathesis would occur as follows:



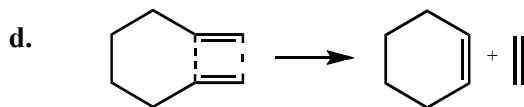
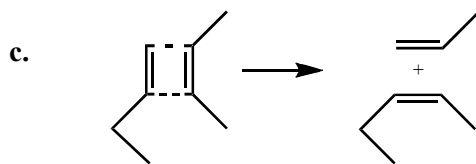
In addition, reactants could undergo self-metathesis, for example



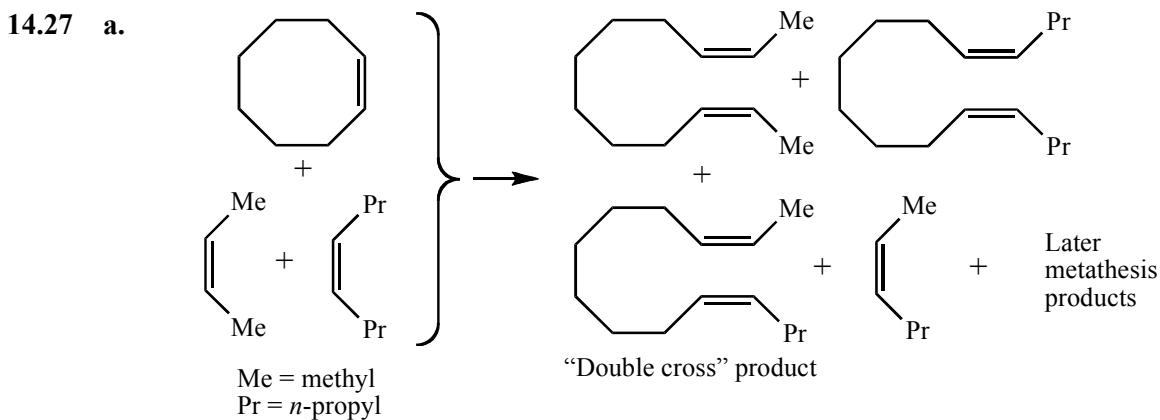
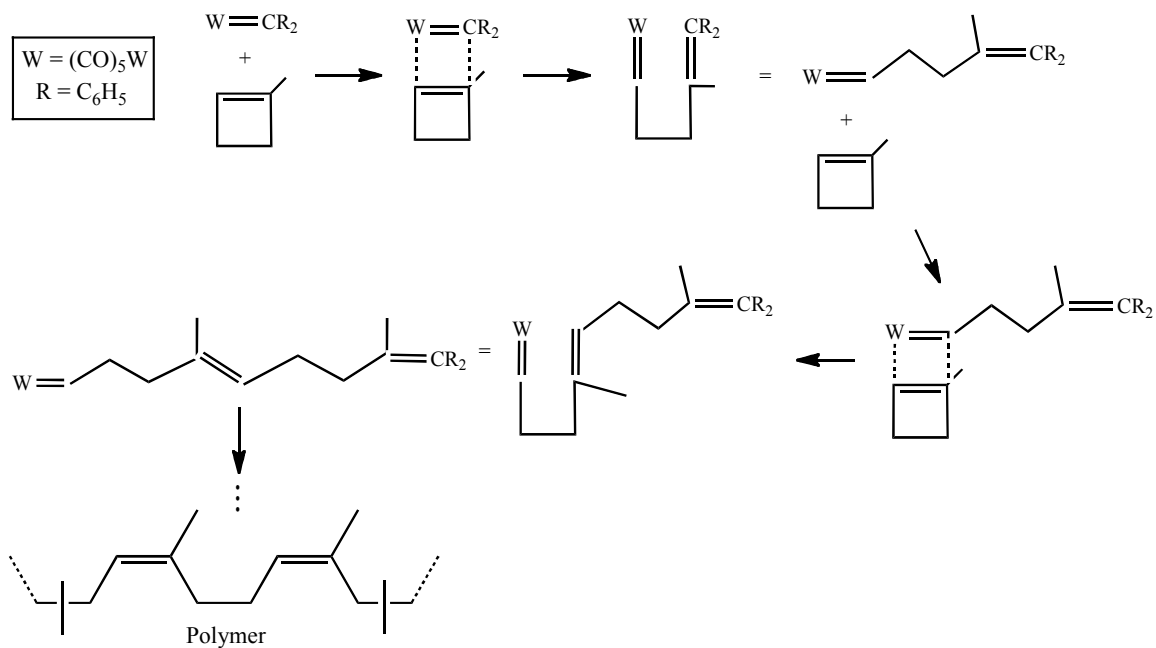
and the products of the direct metathesis could undergo further metathesis to give a variety of products. One of these could be formed as shown here:



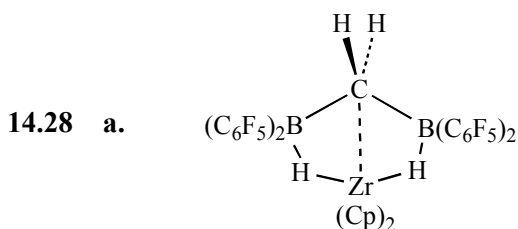
b. This is Hérisson and Chauvin's classic experiment, with products shown in Figure 14.27. As in Part a, self metathesis can also occur, and the products of direct metathesis can also undergo further metathesis to give a variety of products.



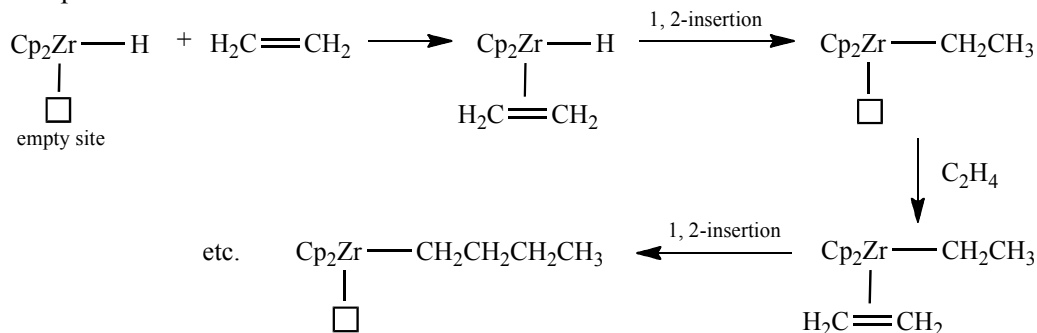
14.26 The catalyst is an 18-electron species with $M = W$. The first steps in the catalytic cycle are diagrammed here:



b. The pairwise mechanism would call for the dimethyl and dipropyl products to be formed first, followed by the “double cross” product. In the non-pairwise mechanism, the double cross product should form simultaneously with the dimethyl and the dipropyl products. Experimental results showed that the double cross product formed (along with the dimethyl and dipropyl products) at the beginning of the reaction, consistent with the non-pairwise mechanism.



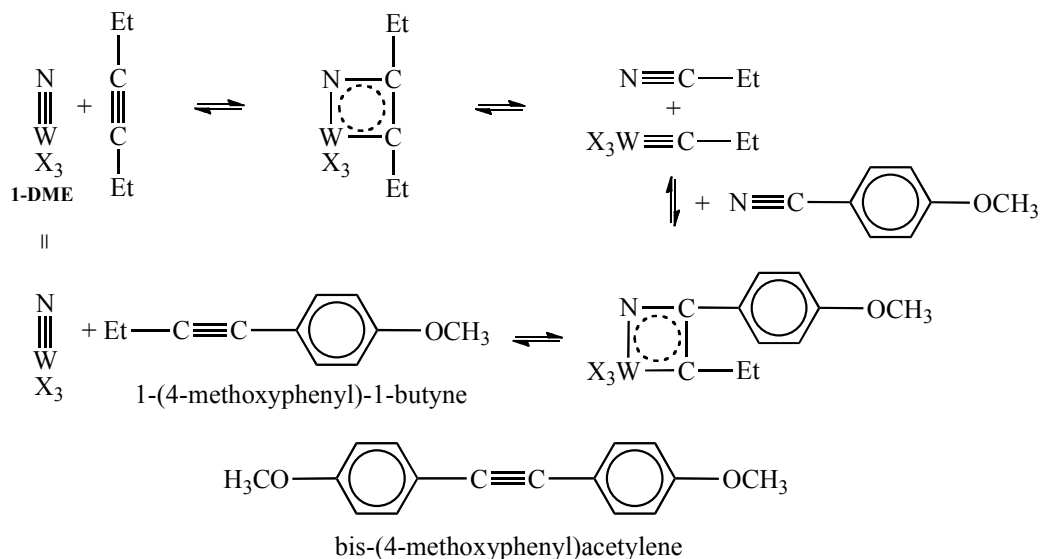
b. One possible route:



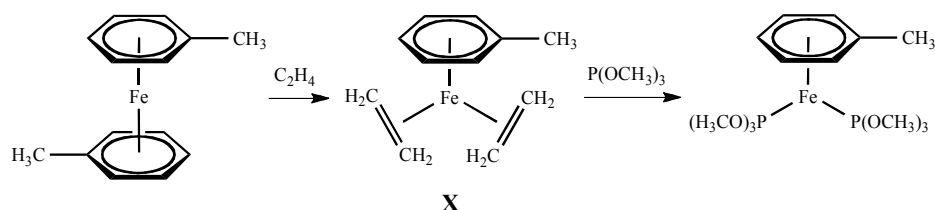
14.29 a. Details of the scheme, together with schematic diagrams of the proposed catalytic cycle and related cycles, are presented in the reference. The catalyst precursor is the 1,2-dimethoxyethane (DME) adduct of $\text{N} \equiv \text{W}(\text{OC}(\text{CF}_3)_2\text{Me})_3$, dubbed **1-DME** (the crystal structure is provided in the reference). Proposed steps include:

1. Reaction of **1-DME** with 3-hexyne to form metallacycle
2. Dissociation of nitrile, leaving tungsten carbyne complex
3. Reaction with *p*-methoxybenzonitrile to form second metallacycle
4. Dissociation of product to regenerate **1-DME**

b. The first product was considered to be 1-(4-methoxyphenyl)-1-butyne, formed as shown below. However, this compound accounted for only 15 mole percent of the reaction products. The major product, bis(4-methoxyphenyl)acetylene, accounting for 77 mole percent of the products, was attributed to secondary metathesis, also involving metallacycle intermediates. The article discusses in detail alternative cycles for forming bis(4-methoxyphenyl)acetylene.



14.30



14.31 $\text{RhCl}_3 \cdot 3 \text{H}_2\text{O} + \text{P}(o\text{-MePh})_3 \longrightarrow \text{I (blue-green)} (\text{C}_{42}\text{H}_{42}\text{P}_2\text{Cl}_2\text{Rh}) \mu_{\text{eff}} = 2.3 \text{ B.M.},$
 $\text{Rh-Cl } \nu = 351 \text{ cm}^{-1}$

I is *trans*- $\text{RhCl}_2(\text{PR}_3)_2$. The IR is the Rh–Cl asymmetric stretch. The *cis* isomer would give two IR bands. One unpaired electron (15 electron species, square planar).

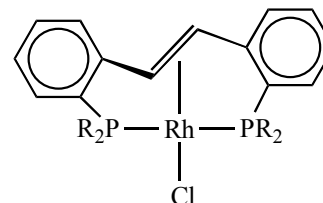
I + heat \longrightarrow **II** (yellow, diamagnetic) $\text{Rh}:\text{Cl} = 1, \nu = 920 \text{ cm}^{-1}$

II Loss of one Cl and combination of two CH_3 's to form a single tridentate phosphine ligand with a π bond. Sixteen electrons around Rh. The double bond in the ligand is perpendicular to the Rh–Cl–P plane because of the size and geometry of the benzene rings.

II + $\text{SCN}^- \longrightarrow$ **III** $\text{Rh}(\text{SCN})$

II:

NMR: δ	Area	Type
6.9–7.5	12	aromatic
3.50	1	doublet of 1:2:1 triplets
2.84	3	singlet
2.40	3	singlet



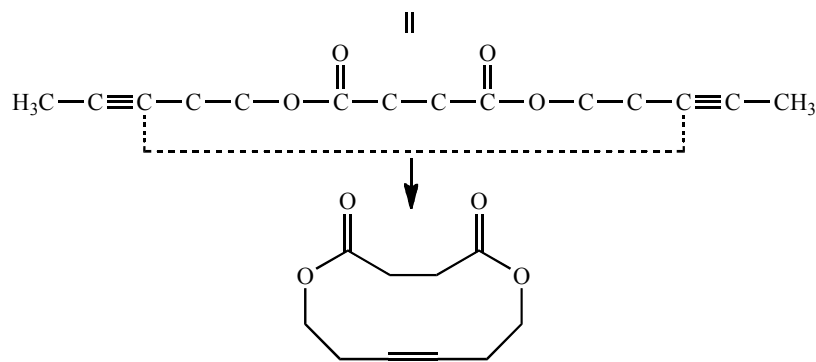
III: Same overall structure as **II**, with SCN substituted for Cl. The singlets are the methyl protons (two separate environments—not obvious from the drawing), the doublet is from the vinylic protons, and the aromatic multiplets are the sum of all the phenyl protons.

II + NaCN \longrightarrow **IV** ($\text{C}_{21}\text{H}_{19}\text{P}$, mw = 604) $\nu = 965 \text{ cm}^{-1}$

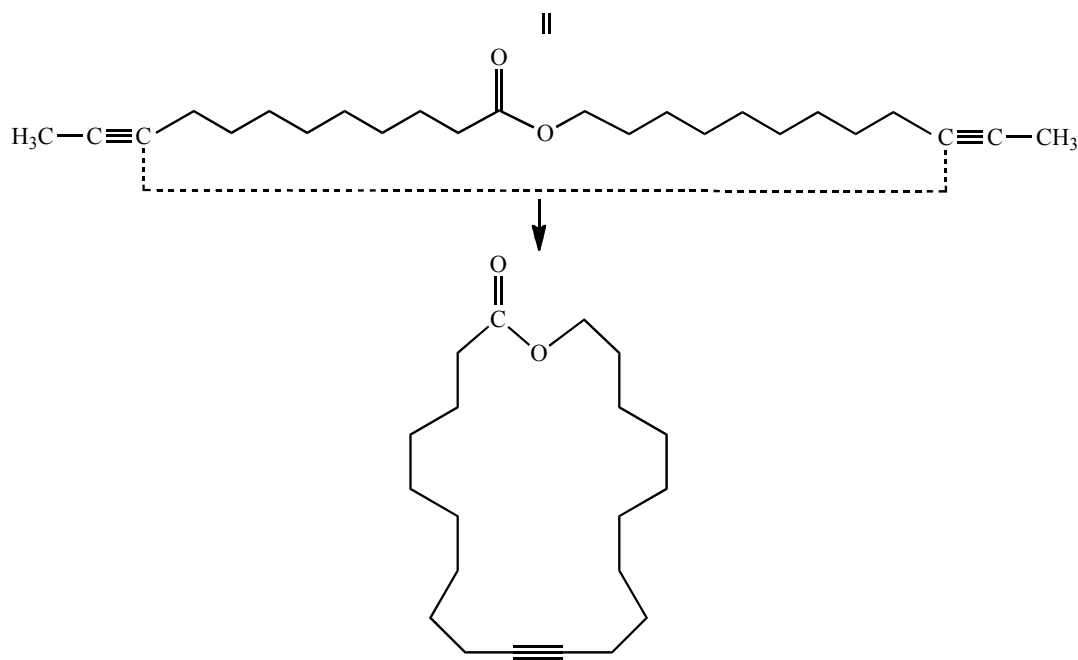
NMR: δ	Area	Type
7.64	1	singlet
6.9 - 7.5	12	aromatic
2.37	6	singlet

IV is the diphosphine ligand, $\text{C}_{42}\text{H}_{38}\text{P}_2$, shown above in compound **II**. (CN^- substitutes for all the ligands in this reaction.) The IR band is characteristic of *trans* vinylic hydrogens. All methyl protons are equivalent in the free ligand (singlet), the vinylic protons are a singlet at 7.64, and the phenyl protons are a multiplet at 6.9–7.5. The change in the vinyl hydrogen IR band shows that the ethylene does coordinate to Rh. Coordination reduces the C=C bonding, which also reduces the C–H bending energy (electrons are drawn away from C–H, toward C–Rh).

14.32 a.

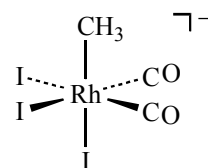


b.



14.33 Evidence in support of the intermediate shown at the right includes:

- (1) An infrared band at 2104 cm^{-1} has been observed. This band is similar to the higher energy band in the Ir analogue, $[\text{CH}_3\text{Ir}(\text{CO})_2\text{I}_3]^-$, which has carbonyl bands at 2102 and 2049 cm^{-1} . A second band, expected for $[\text{CH}_3\text{Ir}(\text{CO})_2\text{I}_3]^-$, would be hidden under strong bands of the reactants and products of steps 2 and 3 of the mechanism.
- (2) The ratio of the absorbance of the 2104 cm^{-1} band to the absorbance of a band at 1985 cm^{-1} of $[\text{Rh}(\text{CO})_2\text{I}_2]^-$, the reactant in step 2, is proportional to the concentration of CH_3I . This is consistent with what would be expected



from the equilibrium constant expression for formation of the intermediate,

$$K = \frac{[\text{Rh}(\text{CO})_2\text{I}_2][\text{CH}_3\text{I}]}{[\text{CH}_3\text{Rh}(\text{CO})_2\text{I}_3]}$$

and is consistent with the steady state approximation for the mechanism.

- (3) The maximum intensity of the 2104 cm^{-1} band occurs when the product of step 3 is formed most rapidly.
- (4) When $^{13}\text{CH}_3\text{I}$ is used, a doublet is observed in the NMR consistent with ^{13}C – ^{103}Rh coupling. Other NMR data also support the proposed structure.

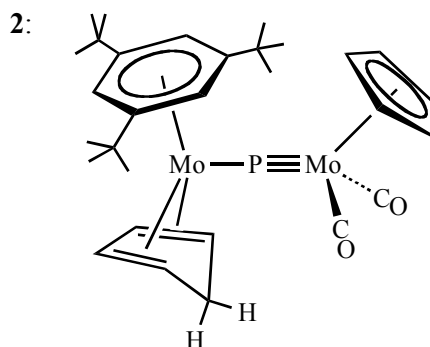
14.34 **A:** $[\text{Fe}(\text{CO})_3(\text{CN})_3]^-$ **B:** $\text{cis}-[\text{Fe}(\text{CO})_2(\text{CN})_4]^{2-}$

The cyanide ion has the capacity to replace ligands such as I^- and CO . The C–N stretch involves a large change in dipole moment, so this vibration, like that of CO , can be useful in characterizing cyano complexes. Because CN has a slightly smaller reduced mass than CO , C–N stretches typically occur at slightly higher energies than C–O stretches (see Section 13.4.1).

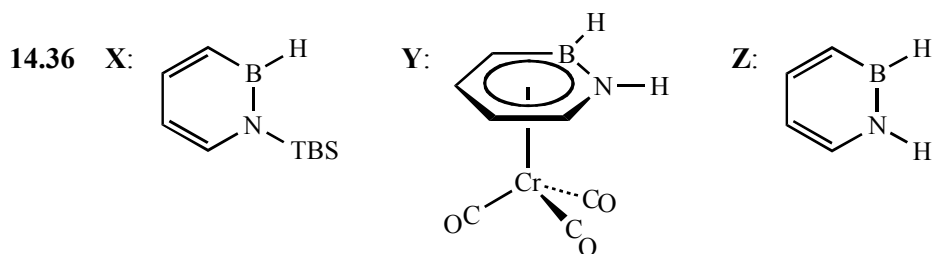
In this situation, both **A** and **B** have two sets of C–N and C–O stretches, indicating that both complexes have at least two of both ligands. As more cyano ligands are added, the concentration of electrons on Fe increases, and both types of ligands become stronger π acceptors, reducing the energy of the stretching vibrations.

The formula of **B** suggests the possibility of both *cis* and *trans* isomers. The observation of two bands in the carbonyl region is consistent with the *cis* isomer. (See also Problem 13.25 and its reference.)

14.35



The two IR bands are as expected for this dicarbonyl complex. NMR peaks can be assigned as follows: chemical shift 5.28 (relative area 5): Cp; 1.31 (27): nine methyl groups on *t*-butyl groups on benzene ring; 5.15 (3): protons on benzene ring; 5.46 (2), 4.22 (2) and hidden small peak: $\eta^4\text{-C}_5\text{H}_6$. In the ^{13}C NMR, the resonance at 236.9 ppm can be assigned to the carbonyl carbons. This product is formed via an unusual attack of a hydride on a cyclopentadienyl carbon; for an additional example of this type of attack, see footnote 17 in the reference.



In heterocycle **Z** coupling of the N–H proton with the ^{14}N nucleus (which has $S = 1$) results in a triplet, and coupling for the B–H proton with the ^{11}B nucleus (which has $S = 3/2$) results in a quartet. (The original spectrum is shown in the reference.)

14.37 See Figure 13.32 for a diagram of this molecular “ferrous wheel”!